CHEMMEDCHEM

CHEMISTRY ENABLING DRUG DISCOVERY

Accepted Article

Title: Discovery of a Potent, Long Acting and CNS Active Inhibitor (BIA 10-2474) of Fatty Acid Amide Hydrolase

Authors: Laszlo Kiss, Alexandre Beliaev, Humberto S. Ferreira, Carla P. Rosa, Maria Joao Bonifacio, Ana I. Lourerio, Nuno M. Pires, Nuno P. Palma, and Patricio Soares-da-Silva

To be cited as: *ChemMedChem* 10.1002/cmdc.201800393

Link to VoR: http://dx.doi.org/10.1002/cmdc.201800393

A Journal of

ChemPubSoc Europe

WILEY-VCH

www.chemmedchem.org

WILEY-VCH

FULL PAPER

Discovery of a Potent, Long Acting and CNS Active Inhibitor (BIA 10-2474) of Fatty Acid Amide Hydrolase

László E. Kiss*[a], Alexandre Beliaev[a], Humberto S. Ferreira[a], Carla P. Rosa[a], Maria João Bonifácio[b], Ana I. Loureiro[b], Nuno M. Pires[b], P. Nuno Palma[b] and Patrício Soares-da-Silva[b,c]

[a] Dr. L. E. Kiss, Dr. A. Beliaev, Dr. H. S. Ferreira, Dr. C. P. Rosa
Laboratory of Chemistry, Department of Research & Development
BIAL – Portela & Cª., S.A.
À Avenida da Siderurgia Nacional, 4745-457 Coronado (S. Romão and S. Mamede), Portugal
E-mail: laszlo.kiss@bial.com

[b] Dr. M. J. Bonifácio, Dr. A. I. Loureiro, Dr. N. M. Pires, Dr. P. N. Palma, Dr. (M.D., Ph.D.) P. Soares-da-Silva
Laboratory of Pharmacology, Department of Research & Development
BIAL – Portela & Cª., S.A.
À Avenida da Siderurgia Nacional, 4745-457 Coronado (S. Romão and S. Mamede), Portugal

[c] Dr. (M.D., Ph.D.) P. Soares-da-Silva
MedInUp - Center for Drug Discovery and Innovative Medicines
University of Porto
Praça Gomes Teixeira, 4099-002 Porto, Portugal

Supporting information for this article is given via a link at the end of the document.

Abstract: Fatty acid amide hydrolase (FAAH) enzyme can be targeted for the treatment of pain associated with various medical conditions. Herein, we report the design and synthesis of a novel series of heterocyclic-*N*-carboxamide FAAH inhibitors that achieve good alignment of potency, metabolic stability and selectivity over monoacylglycerol lipase (MAGL) and carboxylesterases (CEs) enzymes. Lead optimization efforts carried out with benzotriazolyl- and imidazolyl-*N*-carboxamide series led to the discovery of clinical candidate **8l** (3-(1-(cyclohexyl(methyl)carbamoyl)-1*H*-imidazol-4-yl)pyridine 1-oxide; BIA 10-2474) as a potent and long acting inhibitor of FAAH. However, during a Phase I clinical trial with compound **8l**, unexpected and unpredictable serious neurological adverse events occurred affecting five healthy volunteers, including the death of one subject.

Introduction

Fatty acid amide hydrolase (FAAH, EC 3.5.1.99), an integral membrane bound enzyme, is a member of the extensive family of serine hydrolases referred to as amidase signature (AS) family.[1] It catalyses degradation of lipid signalling fatty acid amides including the sleep-inducing oleamide and endogenous cannabinoid anandamide (AEA).[2] AEA binds and activates both central (CB1) and peripheral (CB2) cannabinoid receptors of the endocannabinoid system (ECS).[3] The modulation of levels of AEA via inhibition of FAAH has potentially clinical relevance in a wide range of diseases and pathological conditions. Therefore, both the ECS and FAAH have become recognized as promising therapeutic targets for the treatment of a range of central and peripheral disorders.[4-5] Importantly, phenotypes observed in FAAH knockout mice allowed to expect the efficiency of FAAH inhibitors not being compromised by typical side effects of direct CB1 agonists.[6] Due to increasing interest over the last two decades, numerous small molecule inhibitors of FAAH belonging to various chemical classes have been reported (for recent reviews see[5-10] and references cited therein).

The X-ray crystal structure of the rat catalytically active transmembrane domain-deleted FAAH was first unveiled in 2002, in complex with an irreversible inhibitor (methoxy arachidonyl fluorophosphonate (MAFP)).[11] Later on, an engineered ''humanized'' rat (h/r) FAAH was produced by interconverting the active site residues of rat and human FAAH, using site-directed mutagenesis.[12] This h/rFAAH combined the efficient rFAAH recombinant expression with the inhibitor sensitivity profile of hFAAH, thus greatly facilitating the design of new inhibitors. Since then, a number of inhibitors have been co-crystallized with this form of the enzyme.[12-19]

The most important classes of compounds with different mechanism of action are the reversible inhibitor heterocyclic ketones[20] exemplified by **1** (OL-135), and the irreversible, covalently binding inhibitors such as carbamates[21] (e.g. **2** (URB597)) and ureas[13] (e.g. **3** (PF3845)) (Figure 1). It is interesting to note, that that despite the quite high chemical

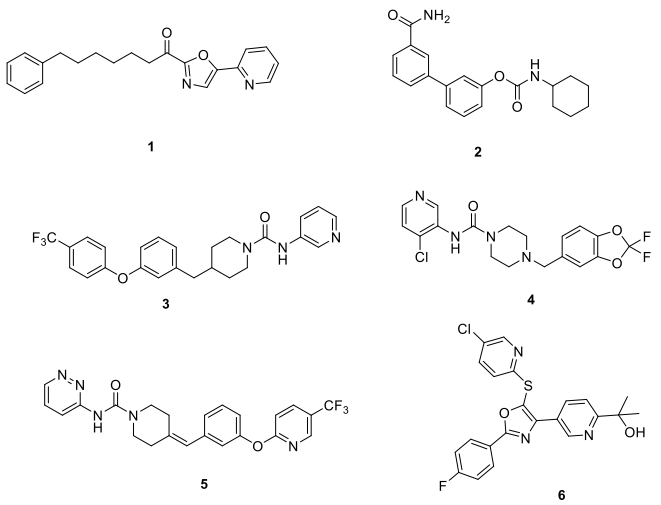

Figure 1. Chemical structure of OL-135 **1**, URB597 **2**, PF3845 **3**, JNJ-42165279 **4**, PF-04457845 **5** and MK-4409 **6**.

stability of the urea functional group in **3**, FAAH is yet inhibited in an irreversible manner by covalently modifying the enzyme's active site.[22] Of the urea class[22-24] the most interesting compounds which have been advanced into clinical trial are **4** (JNJ-42165279)[25] developed by Johnson & Johnson and **5 (**PF-04457845)[26] by Pfizer (Figure 1). Unfortunately, the clinical development of **4** and **5** have been suspended as a precautionary measure following serious safety issues with **8l** (BIA 10-2474) and due to lack of therapeutic effect,[27] respectively. Recent efforts from Merck led to the discovery of oxazole **6** (MK-4409)[28] which has also advanced into clinical development. Compound **6** is described as a reversible FAAH inhibitor but no clinical results published up to now.

Our group set out to design a fast onset, long acting and CNS active FAAH inhibitor, which may be useful for the treatment of pain associated with various medical conditions. Preliminary screening of selected compounds sourced from both commercial vendors and those cherry-picked from our in-house collections for FAAH inhibition led to the identification of the imidazole **8a** (Figure 2, *N*-methyl-*N*-phenyl-1*H*-imidazole-1-carboxamide), which showed moderate in vitro activity (88 % inhibition at a concentration of 10 μM in rat brain homogenates).

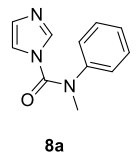

8a

Figure 2. Chemical structure of screening hit **8a**.

At that time, compound **8a** represented a novel scaffold[29] in the field of FAAH inhibitors, although during our research programme a patent application filed by an academic group has independently disclosed similar heterocyclic-*N*-carboxamide scaffolds claiming them as dual inhibitors of MAGL and FAAH enzymes.[30] The structure of **8a** was deemed to be readily amenable to exploration of structure-activity relationships (SAR) and it was therefore selected as the starting point for a medicinal chemistry programme.

Herein, we describe a novel series of potent in vivo CNS active benzotriazolyl- and imidazolyl-*N*-carboxamides that have been designed and synthesized in our laboratory, including **8l** (BIA 10-2474), which in January 2016 faced a severe incident in a Phase I clinical trial, where one person died and others suffered adverse neurological effects.

Results and Discussion

Chemistry

The synthetic routes employed to obtain the initial heterocyclic-*N*-carboxamide inhibitors are outlined in Scheme 1. The necessary dialkylcarbamoyl chloride intermediates were obtained either from commercial sources or prepared by a literature method.[31] The target heterocyclic-*N*-carboxamides were synthesised under two different conditions. More reactive heterocycles such as **7a-d** and **7f** were smoothly carbamoylated with dialkylcarbamoyl chlorides in refluxing tetrahydrofuran (THF) containing base (*N*,*N*-diisopropyl ethyl amine (DIPEA) or pyridine) to provide the target compounds **8a-b**, **8d** and **8f-k** in moderate yield. The 3-pyridyl imidazole analogue **8k** was further oxidized to pyridine *N*-oxide **8l** (BIA 10-2474) on reaction with *meta*-chloroperbenzoic acid (MCPBA) in dichloromethane (DCM) at room temperature. Due to reduced reactivity of **7e** and **9a-b** different reaction conditions were applied for preparing compounds **8c**, **10a**, **10g** and **10o-p**, wherein **7e** and **9a-b** were deprotonated with sodium hydride in THF at 0 °C followed by reaction with the corresponding dialkylcarbamoyl chlorides to give phenyl imidazole **8c** and benzotriazoles **10a**, **10g** and **10o-p** in fairly good yields.

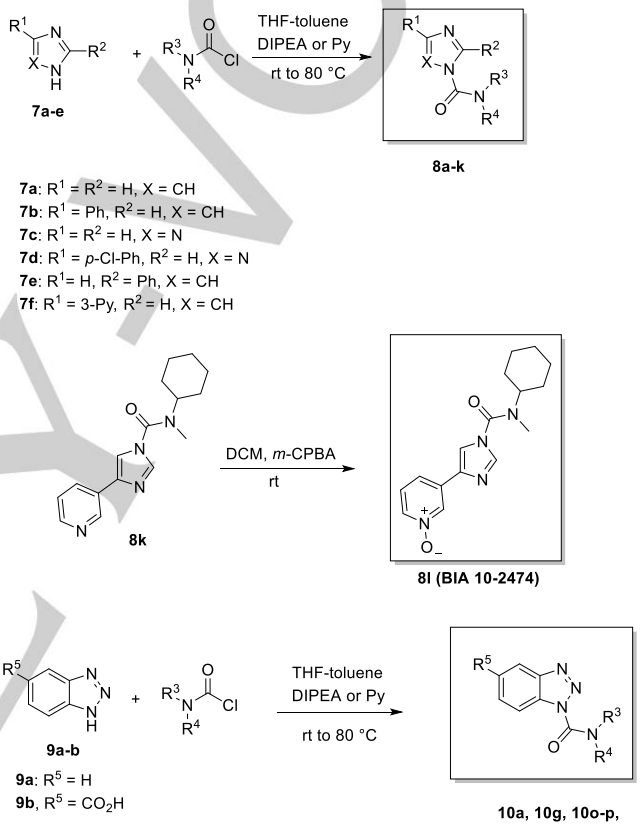

Scheme 1. Preparation of imidazole and benzotriazole analogues

The general synthetic routes to support SAR exploration within the series of *N*-benzotriazolyl carboxamide derivatives are depicted in Scheme 2. Benzotriazoles **9a** and **9c-g** were acylated with 20% toluenic solution of phosgene in THF. Benzotriazole-*N*-carbonyl chloride intermediates thus obtained were treated with secondary amines in THF using pyridine as base to provide the desired *N*,*N*-disubstituted benzotriazole carboxamides (**10b-c**, **10f**, **10h-n**, **11a-c**, **11e-g**) in moderate yield. The carboxamide derivative **11h** was prepared from carboxylic acid intermediate **10p**. Activation of **10p** with thionyl chloride ($SOCl_2$) afforded the corresponding acyl chloride intermediate, which was subsequently reacted with ethanolic ammonia solution to provide **11h**. Mono-substituted benzotriazole *N*-carboxamides **10d-e** were obtained by treating benzotriazole **9a** with isocyanates in DCM at room temperature. Construction of the biphenyl ring in **11d** was accomplished via Suzuki coupling reaction. 6-Bromo

benzimidazole **9b** was smoothly converted to **11d** on the reaction with phenyl boronic acid in a mixture of 1-propanol – water using palladium catalyst ($Pd(PPh_3)_4$) and sodium carbonate as base.

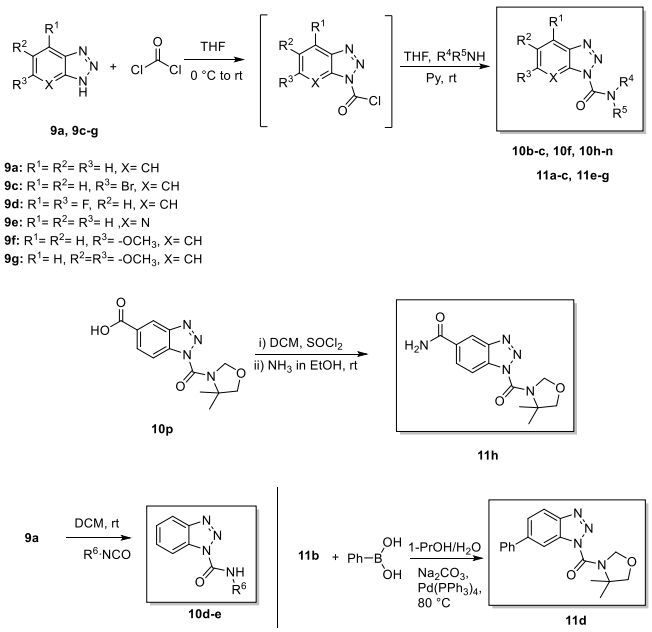

Scheme 2. Preparation of benzotriazole analogues

Pharmacology

In vitro screening of all new compounds was carried out in rat brain membranes. FAAH activity was determined by measuring the formation of ^{3}H-ethanolamine using tritium (^{3}H) labelled AEA as has been described previously.[32]

Table 1. In vitro FAAH inhibition (expressed as percentage of control values) by selected heterocyclic *N*-carboxamide analogues in rat brain homogenates.

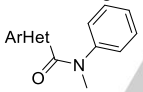

No.	HetAr	10 μM[a]	0.1 μM[a]
8a		12±3	112±20
8b		0±0	84±7
8c		93±6	115±37
8d		0±0	17±2
8e	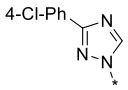	0±0	61±5
10a	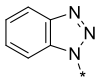	0±0	1±0

[a] % of Control, results are means ± SD (n=4), determined in rat brain homogenates after 15 min of preincubation time.

In the first phase of our hit-to-lead optimization programme, modification by substitution or replacement of the imidazole ring in **8a** with other common heterocycles were investigated. To facilitate the interpretation of the SAR, all prepared analogues shared the same *N*-methylaniline moiety on the right-hand side of the molecule and were evaluated at two different concentrations. The results for a representative selection of compounds are provided in Table 1 and reported in residual enzymatic activity.

Whilst the initial screening hit **8a** exhibited fairly promising activity at a concentration of 10 μM, it was found to be completely inactive at a hundred-fold lower concentration. The 4-phenyl derivative **8b** displayed slightly increased inhibition over the parent **8a**, whereas shifting the phenyl ring to C2 position of the imidazole ring (**8c**) led to drastic reduction in FAAH inhibition. Within the series of heterocycles with three heteroatoms, the unsubstituted 1,2,4-triazole **8d** was found to possess enhanced inhibition over the screening hit **8a**. Inclusion of *p*-chloro-phenyl group at 3-position of the imidazole ring (**8e**) made little difference in potency compared to imidazole analogue **8b**. However, it was then discovered that in vitro inhibition could markedly be enhanced by condensing the triazole core in **8d** with phenyl ring (**10a**). Benzotriazole **10a** was clearly the most potent inhibitor with an IC_{50} of 7 nM, and therefore, it was further studied pharmacologically. Target selectivity of **10a** for FAAH relative to CEs and MAGL enzymes was evaluated in vitro in rat liver microsomes and in rat cerebellum cytosol, respectively. Inhibitor **10a** showed significant selectivity for FAAH (IC_{50} = 7 nM) over CE (IC_{50} > 1 μM) and MAGL (IC_{50} > 100 μM) enzymes, although it inhibited CEs to a greater extent than reference compounds **2** and **3** (Table 2).

In another experiment **2**, **3** and **10a** were assessed for in vivo FAAH inhibition. Compounds were orally administered to overnight fasted mice at a dose of 30 mg/kg, and thereafter at 1h post-administration the FAAH activity was determined. As seen in Table 2, whilst **2** and **3** exhibited over 90 % inhibition in both the liver and brain, compound **10a** only moderately inhibited FAAH both centrally and peripherally. At this point compound **10a** was selected as an early lead for further optimization. The SAR around our lead structure **10a** was investigated by varying the amino side-chain of the carboxamide core structure. Accordingly, we proceeded to synthesize a restricted series of benzotriazoles (**10b-d**) aimed at enhancing in vitro efficacy whilst maintaining good target selectivity over CEs and MAGL. Introduction of electron withdrawing groups (EWGs) such as fluorine in the aromatic ring (**10b**) had no beneficial effect on in vitro inhibitory potency. Increasing the electron density on the aromatic ring in **10a** by appropriate substitution at the *meta* positions led to a weakly active compound (**10c**). Removal of the *N*-methyl group in **10b** completely abolished FAAH inhibition (**10d**). Moreover, compounds **10b-d** inhibited CE and MAGL to an appreciable extent. The next round of SAR concentrated on analogues which

incorporate benzylic, cycloaliphatic and saturated heterocyclic sidechains (**10e-k**). Compounds **10e-k** were evaluated both in vitro (FAAH, CEs and MAGL) and in vivo (30 mg/kg, p.o., mice 1 h post-dose). Despite the promising in vitro FAAH activity of the *N*-benzyl derivative **10e**, only residual in vivo inhibition was seen both centrally and peripherally. In contrast, the in vitro also highly potent *N*-methyl-*N*-benzyl **10f** derivative showed evidence of in vivo efficacy, but it was uninteresting in terms of selectivity.

Table 2. In vitro FAAH, CE, MAGL and in vivo FAAH inhibition (expressed as % of control values) by selected benzotriazole *N*-carboxamides.

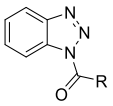

No.	HetAr	100 nM[a,b]	10 nM[a,b]	Liver[a,c]	Brain[a,c]	CEs[a,d]	MAGL[a,e]
2		0±0	15±3	6±1	9±2	72±5	87±4
3		7±4	101±31	2±2	1±0	95±17	87±12
10a	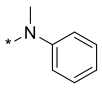	1±0	42±12	34±5	34±9	31±2	73±4
10b	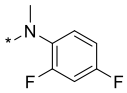	2±1	35±3	ND	ND	40±1	70±6
10c	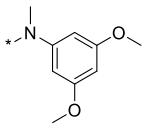	76±0	ND	ND	ND	ND	ND
10d	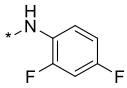	100±5	ND	ND	ND	ND	ND
10e	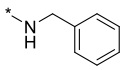	2±1	13±1	84±6	87±7	67±4	4±1
10f	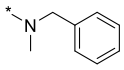	0±0	0±0	6±2	1±0	24±1	2±2
10g		3±0	39±10	41±5	47±2	33±2	10±2
10h	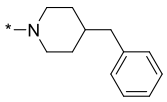	0±0	0±0	6±1	8±1	24±2	7±5
10i	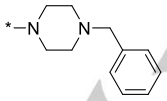	0±0	0±0	15±4	20±5	27±1	7±4
10j	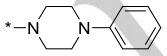	0±0	1±0	30±5	88±7	28±2	12±4
10k	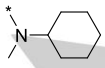	1±2	1±0	1±0	0±0	30±1	73±3
10l	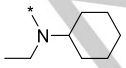	94±12	ND	ND	ND	57±7	80±18
10m	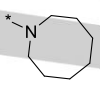	15±1	62±6	ND	ND	30±2	58±6

10n	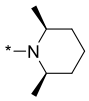	71±7	ND	ND	ND	28±1	35±5
10o		17±3	71±2	ND	ND	60±7	84±25
11a		2±1	78±25	2±1	0±0	81±6	90±5

[a] % of Control, results are means ± SD (n=4). [b] Determined in rat brain homogenates after 15 min of preincubation time. [c] 30 mg/kg, po, in mice, FAAH activity was determined 1 h after administration. [d] $C_{inhib.}$ = 10 μM. in rat liver microsomes. [e] $C_{inhib.}$ = 100 μM in rat cerebellum cytosol.

Morpholine **10g** exhibited weaker inhibitory activity both in vitro and in vivo than **10f** without improving target selectivity. The piperidine **10h** and piperazine analogues **10i-j** exhibited higher in vitro inhibition either than **2** or **3** at a concentration of 10 nM irrespectively of type of substitution. Unfortunately, both CEs and MAGL were inhibited by **10h-j** to high extent. In vivo efficacy of **10h-j** both centrally and peripherally was comparable to that of **2** and **3** with the exception of **10j**, which showed a clear preference for peripheral FAAH. Another effort within the benzotriazole *N*-carboxamide series focused on further functionalization of the amino moiety. We envisioned that compounds endowed with higher steric hindrance in the neighbourhood of the carbonyl group might improve the poor target selectivity of earlier *N*,*N*-dialkyl analogues (**10f-j**) without compromising the excellent in vitro and good in vivo FAAH inhibitory ability. Indeed, this hypothesis was borne out, the in vitro highly potent *N*-methyl-*N*-cyclohexyl derivative **10k** exhibited greater in vivo efficacy over **10f-j** with considerably improved selectivity over MAGL. Thus, compound **10k** exhibited the greatest promise at this point and subsequent efforts focused on this particular *N*-alkyl, *N*-cycloalkyl series, leading to the elaboration of derivatives **10l-n** shown in the lower half of Table 2. Elongation of the *N*-methyl group of **10k** with a methylene spacer resulted in inactive derivative **10l**. Incorporation of eight-membered (**10m**) macrocyclic amines was less tolerated in vitro without providing improvement in selectivity over both MAGL and CEs. A structural isomer of **10m**, which includes 2 methyl groups at 2,6-positions of the piperidine ring (**10n**), was weakly potent in vitro. However, the 5-membred 2,2-dimethyloxazolidine analogue **10o**, which displayed moderate in vitro FAAH inhibition, was endowed with better target selectivity than any other previously synthesized analogue. Moving the two methyl groups to 4-position of the oxazolidine ring to change the steric crowding around the carbonyl group gave **11a**. This compound had slightly higher in vitro FAAH inhibition and improved target selectivity over regioisomer **10o**, but more importantly, demonstrated potent oral activity. On the basis of these findings, **11a** was selected for further pharmacological studies. The IC_{50} of **11a** was calculated to be 19 nM. The dose-dependent central- and peripheral inhibitory ability of **11a** was assessed in the mouse (1 h post-dose) given increasing doses of compound **11a** (0.001-3.0 mg/kg, p.o.).

Table 3. In vitro CYP450 metabolic stability in different species by **11a**, **11h**, **8h** and **8l**.

No.	mouse[a]	rat[a]	dog[a]	primates[a]	human[a]
11a	5±0	26±0	1±0	0±0	52±9
11h	87±9	87±0	101±6	57±3	96±8
8h	62±0	88±6	54±0	41±3	75±4
8l	99±2	91±1	94±2	88±1	95±1

[a] $C_{inhib.}$ = 5 μM in liver microsomes after 1h of incubation, data are given in % of remaining, results are means ± SD (n=4).

Compound **11a** was found to inhibit both peripheral and cerebral FAAH with ED_{50}'s of 7 μg/kg and 61 μg/kg, respectively. Reference compound **3** was a slightly weaker inhibitor of FAAH in the liver than **11a** in the same conditions but in the brain found to be equipotent ($ED_{50(liver)}$ = 23 μg/kg; $ED_{50(brain)}$ = 63 μg/kg). In another experiment, inhibitor **11a** was incubated with liver microsomes (at a concentration of 5 μM) prepared from different species to evaluate the potential likelihood of metabolic instability. Moderate to high metabolism was observed in different species with the highest degradation seen in mouse, primates and dog (Table 3).

Table 4. In vivo FAAH and in vitro CE and MAGL inhibition data (expressed as % of control values) of selected benzotriazole *N*-carboxamides.

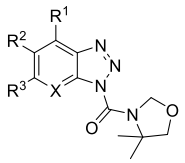

No.	R^1	R^2	R^3	X	Liver[a,b]	Brain[a,b]	CEs(10 μM)[a,c]	MAGL(100 μM)[a,d]	CYPs(50 μM) [e]
2					74±20	91±7	72±5	87±4	ND
3					7±4	5±1	95±17	87±12	ND
11a	H	H	H	CH	10±4	24±7	81±6	90±5	25±2

11b	H	H	Br	CH	16±6	77±29	73±9	67±12	8±2
11c	F	H	F	CH	19±9	71±10	82±5	68±3	8±1
11d	H	H	–Ph	CH	54±6	76±18	92±2	77±4[f]	73±2
11e	H	H	H	N	14±7	12±4	61±11	72±5	ND
11f	H	H	$-OCH_3$	CH	39±7	125±38	79±13	96±1[f]	0±0
11g	H	$-OCH_3$	$-OCH_3$	CH	8±4	9±3	72±5	7±1	55±0
11h	H	$-CONH_2$	H	CH	6±1	6±1	81±7	96±2	67±2

[a] % of Control, results are means ± SD n=4. [b] 0.1 mg/kg, po, in mice, FAAH activity was determined 8 h after administration. [c] In rat liver microsomes. [d] In rat cerebellum cytosol. [e] $^{e}C_{inhib.}$ = 50 μM in mouse liver microsomes after 1 h of incubation, data are given in % of remaining.

Despite the outstanding in vivo efficacy, benzotriazole derivative **11a** was not considered for further development, but it was selected for additional optimization to improve its pharmacological profile. Blocking the 4,4-dimethyl oxazolidinyl moiety in structure of **11a**, further investigation into the effect of the aromatic substitution on CYP450 stability (50 μM, 1 h of incubation) and in vivo efficacy (0.1 mg/kg, p.o., 8h post-dose) were carried out. Table 4 details results for new compounds and includes comparative data for **2** and **3**. Despite the high in vitro potency of **2** (IC_{50} = 5 nM)[33], only residual in vivo FAAH inhibition was observed in both liver and brain (0.1 mg/kg, p.o., 8h post-dose). In contrast, compound **11a** displayed comparable in vivo potency to that of **3** in both liver and brain. Inclusion of bromine (**11b**) atom at C-6 position of the benzotriazole ring provided a metabolically unstable compound and made little difference in in vivo inhibitory profile. The 4,6-difluoro derivative **11c** did not perform better in vivo than the mono bromo derivative **11b** and failed to improve metabolic stability. Incorporation of a bulky phenyl group as in **11d** was found to be detrimental for in vivo potency.

Table 5. In vivo FAAH and in vitro CE and MAGL inhibition data (expressed as % of control values) of selected imidazole *N*-carboxamides.

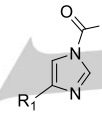

No.	R_1	R_2	100 nM[a,b]	Liver[a,c]	Brain[a,c]	CEs(10 μM)[a,d]	MAGL(100 μM)[a,e]
8b	-Ph	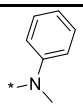	84±7	11±5[f]	14±17[f]	105±5	ND
8f	-Ph		94±10	53±6	92±7	95±6	92±3
8g	-Ph	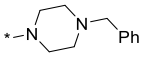	1±0	ND	ND	52±2	61±6
8h	-Ph	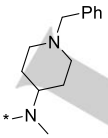	41±7	10±2	11±4	97±8	92±8
8i	-Ph	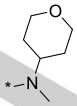	104±18	12±4	38±18	96±7	96±1
8j	-Ph	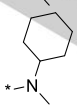	37±3	33±2	86±5	90±11	91±3
8k	3-Py	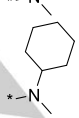	75±7	13±4	75±16	97±3	94±4
8l	3-Py-*N*-oxide	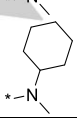	85±11	6±2	8±2	102±5	96±4

[a] % of Control, results are means ± SD (n=4). [b] Determined in rat brain homogenates after 15 min of preincubation time. [c] 0.1 mg/kg, po, in mice, FAAH activity was determined at 8 h after administration. [d] In rat liver microsomes. [e] In rat cerebellum cytosol. [f] 30 mg/kg, po, in mice, FAAH activity was determined at 1 h after administration.

Replacement of the phenyl ring in **11a** with a pyridyl ring gave **11e**, which demonstrated over 85% peripheral and cerebral inhibition with slight increase in inhibition of CEs. As expected, methoxy derivative **11f** was poorly active in vivo most probably due to extensive CYP450 mediated metabolism. Surprisingly, the 5,6-dimethoxy derivative **11g** was endowed with reasonable good metabolic stability and displayed impressive FAAH inhibition, although it is a good inhibitor of MAGL. Finally, the optimal compound from this series was achieved by a simple incorporation of a carboxyamide group at C-5 position of **11a** to produce a compound **11h** with high CNS efficacy and good CYP450 stability in vitro over **11a** in various species (Table 3).

For completeness of the SAR, we considered the replacement of benzotriazole ring in **11h** with other heterocycles such as imidazole and triazole. We were interested to see what sort of pharmacological effect in terms of in vivo efficacy and target selectivity could be expected by this modification. From the early imidazole and triazole inhibitors (Table 1) the latter class was ruled out due to poor selectivity over CEs. Imidazole **8b** was devoid of CEs inhibition and despite the lower in vitro potency, it was endowed with more enhanced in vivo inhibition (30 mg/kg, po, and 1h post-dose) both centrally and peripherally over our initial benzotriazole derivative **10a**. (Table 5). Therefore, we were encouraged to synthesize further imidazole analogues (**8f-g**) for in vitro and in vivo comparison to their benzotriazole counterparts (**10i**, **10j** and **11a**). Compounds that exhibited over 90 % of control in the MAGL and CEs assays were evaluated in vivo in mice (0.1 mg/kg, p.o., 8h post-dose). The results are shown in Table 5. Majority of the newly synthesized compounds were much less efficacious in vitro than their benzotriazole analogues. Compound **8f**, the analogue of **11a**, demonstrated some degree of peripheral inhibition, but centrally was ineffective. Although piperazine analogue **8g** fully abolished FAAH activity at a concentration of 100 nM, somewhat it inhibited both CEs and MAGL. Increasing the steric hindrance near the carbonyl group led to a more selective compound **8h**, which exhibited over 90 % in vivo FAAH inhibition in the brain and liver. Replacement of the *N*-benzyl group (**8h**) with an oxygen atom (**8i**) or methylene group (**8j**) led to a reduction in central inhibition. The more polar and basic pyridyl analogue **8k** failed to improve in vivo efficacy in the brain over the parent **8j**. However, the even more polar pyridine *N*-oxide derivative **8l** displayed impressive inhibition in both brain and liver with no measurable effect in vitro in CEs and MAGL assays. Furthermore, compound **8l** displayed favourable in vitro metabolic stability in various species (Table 3). Generally, we can say that within the imidazole scaffold few correlations could be established between results of in vitro and in vivo FAAH activity. Possible explanations include in vivo accumulation of the inhibitors, which has not been seen (manuscript in preparation) or their interaction with the enzyme might be affected by the enzyme environment in vitro (brain membranes) or in vivo; further studies will be required to understand this effect. Having identified from these series **11h**, **8h** and **8l** possessing excellent in vivo FAAH inhibitory activity (> 90 % of control in brain and liver at a dose of 0.1 mg/kg, p.o.) and good selectivity over CEs and MAGL (> 80 % of control), subsequent experiments with **3**, **8h**, **8l** and **11h** were designed. Figure 3 highlights their FAAH inhibition profile in mouse liver and brain homogenates at a dose of 0.1 mg/kg, p.o. Compounds **3**, **8h**, **8l** and **11h** were found to achieve their maximum inhibitory effect at 1 h post-dose in the liver.

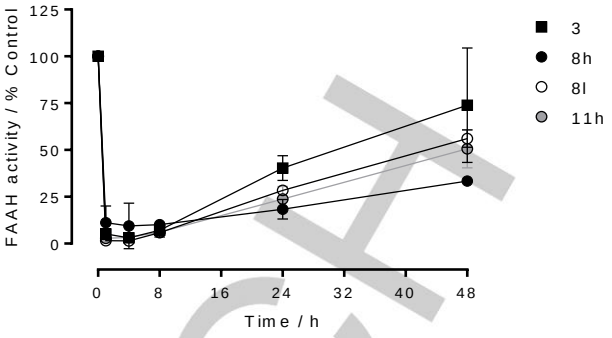

Figure 3. Liver FAAH activity after oral administration of 0.1 mg/kg of compounds **3** (■), **8h** (●), **8l** (○) and **11h** (◉). Results are means ± SD (n = 4).

Thereafter, the constant peripheral inhibition of FAAH (> 90 %) was sustained over the next 7 h, followed by gradual return to lower levels at later time points.

The profile of central inhibition by **3**, **8h** and **8l** was found to be different to that of their liver inhibition. Inhibitors **3**, **8h** and **8l** produced their maximal inhibitory effect (> 90 %) in the brain only at 8 h post dose, and significant central inhibition by **8h** and **8l** (> 50 %) was maintained up to 48 h post-administration (Figure 4). In contrast, compound **11h** displayed similar inhibitory profile (T_{max} = 1 h) both centrally and peripherally and found to achieve long lasting effect.

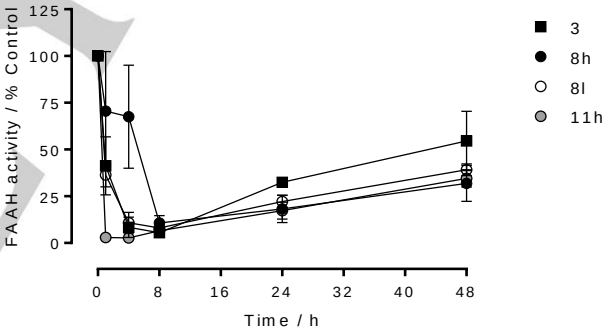

Figure 4. Brain FAAH activity after oral administration of 0.1 mg/kg of compounds **3** (■), **8h** (●), **8l** (○) and **11h** (◉). Results are means ± SD (n = 4).

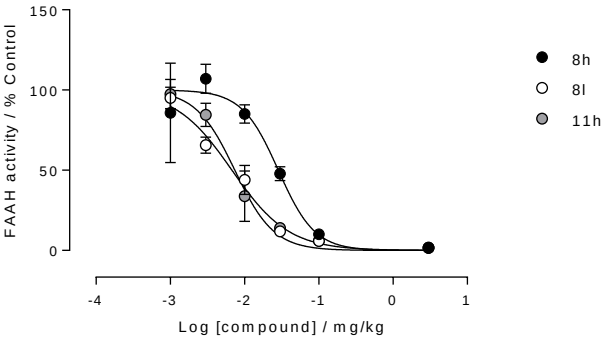

Figure 5. Effect of increasing doses of compounds **8h (●), 8l (○)** and **11h (◉)** on mice liver FAAH activity 8 h after oral administration of each compound. Results are means ± SD (n=4).

Finally, we examined the dose dependent FAAH inhibitory profile by **8h**, **8l** and **11h**. Mice were given increasing doses of

compounds **8h**, **8l** and **11h** ranging from 0.001 to 3 mg/kg p.o., thereafter, at 8 h post-administration the FAAH activity was assayed in liver and brain. The results demonstrate (Figure 5 and 6) that all three compounds were very efficacious in these assays. In the liver compounds **8l** and **11h** are essentially equipotent with ED_{50}'s of 7 µg/kg, whereas inhibitor **8h** was slightly less potent with an ED_{50} value of 28 µg/kg. Again, **11h** was the most potent compound out of **8h**, **8l** and **11h** at inhibiting cerebral FAAH with an ED_{50} value of 14 µg/kg. Imidazoles **8h** and **8l** displayed less marked inhibition with ED_{50}'s of approximately 79 and 27 µg/kg, respectively.

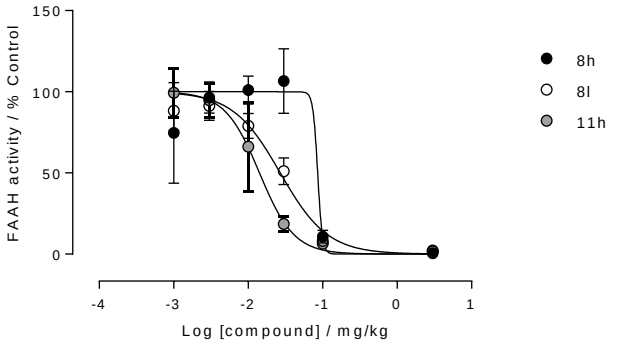

Figure 6. Effect of increasing doses of compounds **8h** (●), **8l** (○) and **11h** (●) on mice brain FAAH activity 8 h after oral administration of each compound. Results are means ± SD (n=4).

The overall pharmacological profiles of **8h**, **8l** and **11h** did not demonstrate marked differences and all three inhibitors were efficacious in the low µg/kg range. Therefore, other factors such as ease of large scale manufacturing and cost of synthesis played a role in preclinical candidate selection.

Our synthetic feasibility analysis revealed difficulties in synthesis of **11h**. Any kind of 1*H*-benzotriazole compound substituted at 5-position exist in three tautomeric forms, which may result in different products in the carbamoylation step. Indeed, **11h** was always contaminated with the unwanted regioisomer (substituted at 6-position of the benzotriazole ring) and isolation of a pure sample of **11h** was not really feasible by a simple recrystallization. In contrast, the most efficacious imidazole compound **8l** could easily be prepared from cheap raw materials in a simple few steps process.[34] Furthermore, inhibitor **8l** was screened against a panel of 97 off-targets (Caliper Life Sciences), including neurotransmitter related targets, ion channels, prostaglandins, growth factors/hormones, peptides and enzymes and at a concentration of 10 µM none of those off-targets was found to be inhibited/blocked by **8l** (see supporting information). Therefore, compound **8l** was selected as preclinical candidate and later on advanced into Phase I clinical studies.

Conclusions

A novel series of potent benzotriazolyl- and imidazolyl-*N*-carboxamides have been developed from an in vitro imidazolyl-*N*-carboxamide hit **8a**. The 4,4-dimethyloxazolidinyl derivative **11a** was the most potent compound from this series with limited in vitro metabolic stability in different animal species. Consequently, the carboxamide substituted derivative **11h** was prepared and found to be highly efficacious in the CNS, metabolically stable and devoid of off-target effects (CEs and MAGL). Further optimization resulted in other selective (CEs and MAGL) in vivo potent imidazolyl *N*-carboxiamides such as **8h** and **8l**. On the basis of overall pharmacological profile, inhibitor **8l** was selected for clinical development. Since the accident in the clinical trial concerning **8l** in which one person died and four were hospitalised with neurological symptoms[35] there has been much speculation as to its cause. The investigations conducted by the French authorities concluded that it was an unexpected effect of the test item, having ruled out other extraneous causes. Their conclusion was that the accident was likely to have been caused by an unknown off-target effect of **8l**.[36] However, the nature of this off-target effect remains obscure, although much speculation has centred around the idea that **8l** is not particularly selective for the FAAH enzyme. In fact, a recent activity-based profiling of serine hydrolases revealed that **8l** inhibited not only FAAH, but ABHD6 and some other serine hydrolases namely FAAH2, CES1, CES2, CES3, ABHD11, LIPE, and PNPLA6 albeit at concentrations several folds higher than those needed for FAAH inhibition.[37] Although the published data provide information about the selectivity of **8l**, it does not allow to conclude which of the identified off-targets could be responsible for the toxicity found. Even in the case of PNPLA6, which has previously been linked to organophosphate-based neurotoxicity in humans, it was shown that carbamoylation of the enzyme (expected effect of **8l**) was not neuropathic.[38] Detailed pharmacological characterization of the clinical candidate **8l** will be addressed in a separate publication including a discussion on off target effects, in addition to the preliminary data already disclosed.[39-41] Preliminary information concerning the safety profile of **8l** during clinical trial BIA-102474-101 have been provided, the conclusions drawn already revealed that 1) following multiple-ascending-doses up to 20 mg, Inhibitor **8l** was found to be safe and well tolerated and systemic exposure to anandamide increased in a dose dependent manner[42] and 2) five out of six subjects exposed to **8l** at 50 mg/day reported unexpected CNS related serious adverse events, for which causality cannot be excluded; the available data does not allow discerning about specific reasons that could have caused the SAEs, which were considered unexpected and unpredictable.[43]

Experimental Section

Chemistry

NMR spectra were recorded on a Bruker Avance III (600 MHz) Spectrometer with solvent used as internal standard, and data are reported in the order: chemical shift (ppm), number of protons, multiplicity (s, singlet; d, doublet; dd, doublet of doublet; t, triplet; q, quartet; m, multiplet; br, broad), approximate coupling constant (J) in Hertz and assignment of a signal. Elemental analyses were performed on a CE Instruments, EA 1110 CHNS analyser. The purity of the compounds in all cases was higher than 95%. Analytical TLC was performed on precoated silica gel plates (Merck 60 Kieselgel F 254) and visualized with UV light. Solvents and reagents were purchased from Aldrich, Merck and Fluka and were used without further purification.

***N*-Methyl-*N*-phenyl-1*H*-imidazole-1-carboxamide (8a).** To a stirred solution of imidazole **7a** (681 mg, 10 mmol) in THF (15 mL) at 0 ºC was added a solution of methyl(phenyl)carbamic chloride (848 mg, 5 mmol) in toluene (6 mL). After being stirred for 2 h at room temperature, the reaction was filtered and the filtrate was evaporated. Chromatography (in DCM) followed by trituration with diethyl ether afforded **8a** as a white powder (446

mg, 44%), mp.: 58 °C. ^{1}H NMR ($CDCl_3$): δ 7.57 (1H, s), 7.39 (2H, t, *J* = 7.7 Hz), 7.32 (1H, t, *J* = 7.3 Hz), 7.13 (2H, d, *J* = 7.7 Hz), 6.85 (1H, s), 6.81 (1H, s), 3.50 (3H, s). ^{13}C NMR ($CDCl_3$): δ150.2, 142.9, 137.7, 130.3, 129, 128, 125.9, 118.4, 40.1. Elemental analysis: ($C_{11}H_{11}N_3O$): Calc: C, 65.66; H, 5.51; N, 20.88. Found: C, 65.68; H, 5.11; N, 21.03.

***N*-Methyl-*N*,4-diphenyl-1*H*-imidazole-1-carboxamide (8b).** To a stirred solution of 4-phenyl-1*H*-imidazole **7b** (433 mg, 3.0 mmol) in THF (10 mL) was added DIPEA (0.78 mL, 4.5 mmol) followed by a solution of methyl(phenyl)carbamic chloride (534 mg, 3.15 mmol) in toluene (4 mL). The reaction mixture was stirred at room temperature for 1 h, then was heated at 80 °C for 1 h. After being cooled to room temperature the reaction was evaporated and partitioned between DCM and water. The organic layer was separated, dried over $MgSO_4$, filtered and evaporated. Trituration in a mixture of petroleum ether–ethyl acetate (3:1) followed by filtration and drying gave **8b** as a beige powder (465 mg, 56%), mp.: 104-105 °C. ^{1}H NMR ($CDCl_3$): δ 7.60 (2H, d, J = 7.7 Hz), 7.53 (1H, s), 7.40 (2H, t, J = 7.7 Hz), 7.34 (1H, m), 7.32 (2H, t, J = 7.6 Hz), 7.25 (1H, m), 7.19 (2H, m), 7.18 (1H, s), 3.52 (3H, s). ^{13}C NMR ($CDCl_3$): δ150.1, 142.9, 141.4, 137.7, 132.8, 130.4, 128.5, 128.2, 127.4, 126, 125, 113.5, 40.2. Elemental analysis: ($C_{17}H_{15}N_3O$): Calc: C, 73.63; H, 5.45; N, 15.15. Found: C, 73.25; H, 5.29; N, 15.05.

***N*-Methyl-*N*,2-diphenyl-1*H*-imidazole-1-carboxamide (8c).** To a stirred suspension of sodium hydride (166 mg, 4.15 mmol, 60% dispersion in mineral oil) in THF (10 mL) at 0 ºC was added a solution of 2-phenyl-1*H*-imidazole **7e** (500 mg, 3.47 mmol) in tTHF (5 mL). The mixture was stirred in the cold for 30 min then was allowed to stir at room temperature for 2 h. The mixture was cooled again to 0 ºC and a solution of methyl(phenyl)carbamic chloride (616 mg, 3.63 mmol) in THF (5 mL) was added dropwise. The reaction was stirred in the cold for 0.5 h, then was allowed to stir at room temperature for 2 days. Thereupon, water was added at 0 ºC and the solvent was evaporated and then the oily residue was partitioned between DCM and water. The organic phase was separated, washed with water and brine, then dried over $MgSO_4$, filtered and evaporated to leave an oily solid. Chromatography (petroleum ether–ethyl acetate, 2:1) allowed the separation of the product as a pale yellow solid (166 mg, 17%), mp.: 123-125 °C. ^{1}H NMR ($CDCl_3$): δ 7.43-7.24 (6H, m), 7.14-6.93 (4H, m), 6.33 (2H, br), 3.37 (3H, s br). ^{13}C NMR ($CDCl_3$): δ 151.9, 146.5, 141.4, 130.3, 129.3, 129, 128.9, 128.3, 127.3, 126.9, 124.1, 120, 38.9. Elemental analysis: ($C_{17}H_{15}N_3O$): Calc: C, 73.63; H, 5.45; N, 15.15. Found: C, 73.83; H, 5.74; N, 14.82.

***N*-Cyclohexyl-*N*-methyl-4-(pyridin-3-yl)-1*H*-imidazole-1-carboxamide (8k).** To a stirred suspension of 3-(1*H*-imidazol-4-yl)pyridine dihydrochloride **7f** (0.654 g, 3 mmol) in THF (10 mL) was added potassium *tert*-butoxide (0.673 g, 6.00 mmol) and the mixture was refluxed for 1 h. Then, *N*,*N*-dimethyl formamide (1 mL) was added and the heating was continued for additional 30 min The resultant brown suspension was cooled to room temperature and treated with pyridine (0.37 mL, 4.50 mmol) and *N*,*N*-dimethylpyridin-4-amine (0.037 g, 0.300 mmol) followed by addition of cyclohexyl(methyl)carbamic chloride (0.553 g, 3.15 mmol). The reaction was heated to 90 °C overnight. After cooling the mixture was diluted with water and extracted with ethyl acetate. The organic phase was dried over $MgSO_4$ and filtered. After evaporation, the crude product was recrystallized from 2-propanol, crystals were collected and dried under vacuum to afford **8k** (62 mg, 6.9 % yield). mp.: 161-163 °C. 1H NMR ($CDCl_3$): δ 9.01 (1H, d d, J = 0.8, 2.3 Hz), 8.53 (1H, d d, J = 1.7, 4.8 Hz), 8.12 (1H, d d d, J = 1.8, 2.2, 8.0 Hz), 7.94 (1H, d, J = 1.3 Hz), 7.58 (1H, d, J = 1.3 Hz), 7.34 (1H, d d d, J = 0.8, 4.9, 8.0 Hz), 3.95 (1H, m), 3.01 (3H, s), 1.87 (4H, m), 1.71 (1H, d br, J = 13.5 Hz), 1.59 (2H, d q, J = 3.5, 12.5 Hz), 1.38 (2H, t q, J = 3.5, 13.0 Hz), 1.13 (1H, t q, J = 3.5, 13.5 Hz). 13C NMR ($CDCl_3$): δ151, 148.5, 146.7, 139.2, 137.3, 132.4, 129, 123.6, 114, 57.6, 31.4, 30, 25.4, 25.2. Elemental analysis: ($C_{16}H_{20}N_4O$): Calc: C, 67.58; H, 7.09; N, 19.7. Found: C, 66.77; H, 7.36; N, 19.95.

3-(1-(Cyclohexyl(methyl)carbamoyl)-1*H*-imidazol-4-yl)pyridine 1-oxide (8l). To a stirred solution of *N*-cyclohexyl-*N*-methyl-4-(pyridin-3-yl)-1*H*-imidazole-1-carboxamide **8k** (90 mg, 0.317 mmol) was added MCPBA (149 mg, 0.475 mmol) at 20-25 ºC in one portion. The reaction was allowed to stir at 20-25 ºC for 20 h. The mixture was evaporated to dryness, the residue was then triturated in diethyl ether. The resulting white crystals were collected, dried on air and recrystallized from isopropanol to afford **8l** (46 mg, 48% yield). mp.: 227.5 °C. ^{1}H NMR ($DMSO_{d6}$): δ 8.70 (1H, t, J = 1.5 Hz), 8.28 (1H, s), 8.20 (1H, s), 8.11 (1H, d, J = 6.5 Hz), 7.78 (1H, d, J = 8.1 Hz), 7.45 (1H, d d, J = 6.5, 8.1 Hz), 3.80 (1H, m), 2.92 (3H, s), 1.77 (4H, m), 1.56 (3H, m), 1.30 (2H, m), 1.11 (1H, m). ^{13}C NMR ($DMSO_{d6}$): δ DMSO: 150.4, 138.3, 137.1, 135.7, 134.7, 132.8, 126.7, 121.2, 117, 56.8, 31.4, 29, 25.1, 24.8. Elemental analysis: ($C_{16}H_{20}N_4O_2$): Calc: C, 63.98; H, 6.71; N, 18.65. Found: C, 63.76; H, 6.94; N, 18.74.

(4,4-Dimethyloxazolidin-3-yl)(4-phenyl-1*H*-imidazol-1-yl)methanone (8f). To a stirred solution of 4-phenyl-1*H*-imidazole **9b** (433 mg, 3.00 mmol) in THF (10 mL) at 0 ºC was added dropwise a solution of 4,4-dimethyloxazolidine-3-carbonyl chloride (515 mg, 3.15 mmol) in THF (10 mL) followed by pyridine (0.48 mL, 5.93 mmol). The reaction was allowed to stir at room temperature for 1 h, then heated at reflux for 4 h. The mixture was cooled to room temperature and evaporated. The residue was partitioned between DCM and water. The organic phase was separated, washed with 2N HCl, water and brine, then dried over $MgSO_4$, filtered and evaporated in vacuum. Column chromatography (petroleum ether–ethyl acetate, 2:1) followed by recrystallization from isopropanol afforded the title compound as a white powder (120 mg, 14 %). mp.: 89 °C. ^{1}H NMR ($CDCl_3$): δ 7.96 (1H, d, J = 1.3 Hz), 7.79 (2H, m, J = 8.3 Hz), 7.52 (1H, d, J = 1.3 Hz), 7.41 (2H, m, J = 7.9 Hz), 7.30 (1H, m, J = 7.3 Hz), 5.13 (2H, s), 3.88 (2H, s), 1.62 (6H, s). ^{13}C NMR ($CDCl_3$): δ 146.5, 142.6, 136.2, 132.7, 128.7, 127.7, 125.2, 112, 81.1, 80.3, 61.8, 22.8. Elemental analysis: ($C_{15}H_{17}N_3O_2$): Calc: C, 66.40; H, 6.32; N, 15.49. Found: C, 65.59; H, 6.35; N, 15.32.

***N*-(2,4-Difluorophenyl)-*N*-methyl-1*H*-benzo[*d*][1,2,3]triazole-1-carboxamide (10b).** To a stirred solution of phosgene (15 mL, 28.5 mmol, 20 % solution in toluene) at 0 ºC was added a solution of 1*H*-benzo[*d*][1,2,3]triazole **9a** (1 g, 8.39 mmol) in THF (20 mL) dropwise. The resulting mixture was stirred in the cold for 0.5 h, then allowed to stir at room temperature overnight. A strong stream of nitrogen was bubbled through the mixture for 0.5 h, then the solvent was removed by evaporation under reduced pressure to give the intermediate 1*H*-benzo[*d*][1,2,3]triazole-1-carbonyl chloride as a clear oil that solidified on standing (762 mg, 4.2 mmol). The above intermediate was suspended in THF (20 mL), cooled to 0 ºC and treated with pyridine (0.36 mL, 4.41 mmol) followed by dropwise addition of 2,4-difluoro-*N*-methylaniline (601 mg, 4.20 mmol). The reaction mixture was allowed to stir at room temperature overnight, then cooled to 0 ºC, diluted with water and ethyl acetate. The organic layer was separated, washed with 1N HCl and brine, then dried over $MgSO_4$ filtered and evaporated. Recrystallization from isopropanol gave **10b** as a white solid (378 mg, 31%), mp.: 91-92 °C. ^{1}H NMR ($CDCl_3$): δ 8.10 (1H, d, J = 8.4 Hz), 8.01 (1H, d, J = 8.1 Hz), 7.63 (1H, m, J = 7.8 Hz), 7.45 (1H, t, J = 7.7 Hz), 7.30 (1H, m), 6.88 (1H, m), 6.84 (1H, m), 3.60 (3H, s). ^{13}C NMR ($CDCl_3$): δ161.8 (d d, J = 11.5, 251.0 Hz), 157.7 (d d, J = 12.5, 252.0 Hz), 150.1, 144.9, 132.7, 129.6, 129.3 (d d, J = 1.5, 10.0 Hz), 127.7 (d d, J = 5.0, 12.0 Hz), 125.4, 119.9, 113.5, 112.1 (d d, J = 4.0, 23.0 Hz), 105.1 (d d, J = 24.0, 26.5 Hz), 39.7. Elemental analysis: ($C_{14}H_{10}F_2N_4O$) Calc: C, 58.33; H, 3.5; N, 19.44. Found: C, 58.66; H, 3.52; N, 19.75.

***N*-(2,4-Difluorophenyl)-1*H*-benzo[*d*][1,2,3]triazole-1-carboxamide (10d).** To an ice-cooled stirred solution of benzotriazole **9a** (300 mg, 2.52 mmol) in DCM (18 mL) was added 2,4-difluoro-1-isocyanatobenzene (410 mg, 2.64 mmol) dropwise. After being stirred for 6 h at room temperature the solvent was evaporated. Recrystallization from a mixture of isopropanol-DCM afforded **10d** as a white solid (209 mg, 30%), mp.:148-150 °C. ^{1}H NMR ($CDCl_3$): δ 9.28 (1H, s), 8.32 (1H, m, J = 8.3 Hz), 8.27 (1H, m, J = 6.0, 8.9 Hz), 8.17 (1H, m, J = 8.3 Hz), 7.70 (1H, m, J = 8.2 Hz), 7.53 (1H, m, J = 8.1 Hz), 7.0 (2H, m). ^{13}C NMR ($CDCl_3$): δ160.6 (d d, J = 11.5, 248.0 Hz), 153.4 (d d, J = 12.0, 249.0 Hz), 146.5, 146.4, 131.5, 130.5,

125.9, 122.7 (d d, J = 2.0, 9.3 Hz), 121.0 (d d, J = 3.7, 11.0 Hz), 120.4, 113.8, 111.6 (d d, J = 4.0, 22.5 Hz), 104.2 (d d, J = 22.5, 27.0 Hz). Elemental analysis: ($C_{13}H_8F_2N_4O$) Calc: C, 56.94; H, 2.94; N, 20.43. Found: C, 56.86; H, 3.09; N, 20.73.

1-(4,4-Dimethyloxazolidine-3-carbonyl)-1*H*-benzo[*d*][1,2,3]triazole-5-carboxylic acid (10p). To an ice-cooled stirred suspension of sodium hydride (7.66 g, 192 mmol) in THF (100 mL) was added a solution of 1*H*-benzo[*d*][1,2,3]triazole-5-carboxylic acid **9b** (12.5 g, 77 mmol) in a mixture of THF (280 mL) and DMF (160 mL) dropwise. The suspension was allowed to stir at room temperature for 0.5 h followed by dropwise addition of 4,4-dimethyloxazolidine-3-carbonyl chloride (13.16 g, 80 mmol) in THF (50 mL) at 0 ºC. The reaction mixture was allowed to stir at room temperature for 5 h. Thereupon, water was carefully added at 0 ºC, the THF was evaporated, then 2N HCl was added until pH 2 was reached. The resulting acidic aqueous phase was extracted three times with a mixture of DCM-isopropanol (7:3). The combined organic layers were dried over $MgSO_4$ and evaporated. The obtained mobile liquid was azeotroped with toluene to leave a brown oil. Purification by column chromatography in a mixture of DCM-methanol (95:5) afforded **10p** as a beige solid (1.8 g, 34%). ^{1}H NMR ($DMSO_{d6}$): δ 8.71 (1H, d d, J = 0.8, 1.3 Hz), 8.26 (1H, s br), 8.21 (1H, d, J = 1.3, 8.6 Hz), 8.16 (1H, d d, J = 0.8, 8.6 Hz), 7.63 (1H, s br), 5.43 (2H, s), 3.90 (2H, s), 1.58 (6H, s). ^{13}C NMR ($DMSO_{d6}$): δ 166.9, 145.4, 144.6, 133.7, 131.9, 129.1, 119, 113.9, 81.7, 78.7, 61.7, 22.5.

(6-Bromo-1*H*-benzo[*d*][1,2,3]triazol-1-yl)(4,4-dimethyloxazolidin-3-yl)methanone (11b). Compound **11b** was prepared by reaction of 6-bromo-1*H*-benzo[*d*][1,2,3]triazole-1-carbonyl chloride (2.63 g, 10.10 mmol) with 4,4-dimethyloxazolidine (1.5 mL, 10.60 mmol, 75% solution in water) as described for **10b**. Recrystallization from ethanol afforded the title product as a beige solid (253 mg, 7.7%), mp.: 119-121 °C. ^{1}H NMR ($CDCl_3$): δ 8.48 (1H, s br), 7.96 (1H, d, J = 8.7 Hz), 7.59 (1H, d d, J = 1.5, 8.7 Hz), 5.53 (2H, s), 3.90 (2H, s), 1.68 (6H, s). ^{13}C NMR ($CDCl_3$): δ145.7, 144.1, 133.7, 129.3, 124.2, 120.8, 117.5, 82.4, 79.5, 62.4, 22.9. Elemental analysis: ($C_{12}H_{13}BrN_4O_2$) Calc: C, 44.33; H, 4.03; N, 17.23. Found: C, 44.08; H, 4.05; N, 17.21.

(4,4-Dimethyloxazolidin-3-yl)(6-phenyl-1*H*-benzo[*d*][1,2,3]triazol-1-yl)methanone (11d). To a stirred suspension of 6-bromo-1*H*-benzo[*d*][1,2,3]triazol-1-yl)(4,4-dimethyloxazolidin-3-yl)methanone **11b** (0.300 g, 0.92 mmol), phenyl boronic acid (0.12 g, 0.97 mmol) and sodium carbonate (0.55 mL, 1.11 mmol) in a mixture of 1-propanol (3.4 mL) and water (0.7 mL) at room temperature was added Tetrakis(triphenylphosphine) palladium(0) (53 mg, 0.046 mmol). The resulting yellow mixture was stirred at 90 ºC for 2 h, then cooled to room temperature and a second crop of tetrakis(triphenylphosphine) palladium(0) (20 mg, 0.16 mmol) was added. The reaction mixture was allowed to stir for further 2h at 90 °C. After cooling to room temperature, the solvent was removed under reduced pressure. The residue was dissolved in ethyl acetate and the organic phase was washed with water. The organic phase was dried over $MgSO_4$, filtered and evaporated to leave a yellow oil. Purification by column chromatography in a mixture of (petroleum ether–ethyl acetate, 20:1) followed by recrystallization from isopropanol afforded the title compound **11d** as a white solid (72 mg, 24%), mp.: 146-147 °C. ^{1}H NMR ($CDCl_3$): δ 8.44 (1H, d d, J = 1.7, 1.6 Hz), 8.14 (1H, d d, J = 0.7, 8.7 Hz), 7.74 (1H, d d, J = 1.6, 8.7 Hz), 7.71 (2H, m, J = 8.2 Hz), 7.50 (2H, m, J = 7.9 Hz), 7.42 (1H, m, J = 7.5 Hz), 5.57 (2H, s), 3.92 (2H, s), 1.70 (6H, s). ^{13}C NMR ($CDCl_3$): δ146.2, 144.7, 143.1, 140.2, 133.5, 128.9, 128.1, 127.9, 125.7, 119.9, 112.4, 82.5, 79.6, 62.2, 23. Elemental analysis: ($C_{18}H_{18}N_4O_2$) Calc: C, 67.07; H, 5.63; N, 17.38. Found: C, 66.92; H, 5.62; N, 17.67.

1-(4,4-Dimethyloxazolidine-3-carbonyl)-1*H*-benzo[*d*][1,2,3]triazole-5-carboxamide (11h). To a stirred solution of 1-(4,4-dimethyloxazolidine-3-carbonyl)-1*H*-benzo[*d*][1,2,3]triazole-6-carboxylic acid **10p** (0.76 g, 2.63 mmol) and pyridine (0.70 mL, 8.67 mmol) in DCM (17 mL) was added thionyl chloride (0.63 mL, 8.67 mmol) dropwise at room temperature. The obtained yellow solution was allowed to stir at room temperature for 15 min followed by dropwise addition to a 1.75M ethanolic solution of ammonia (15 mL, 26.3 mmol) at 0 ºC. The reaction mixture was stirred at room temperature for 0.5 h. Thereupon, water was added and the ethanol was evaporated under reduced pressure. The resulting aqueous phase was extracted with DCM. The organic layer was separated, washed with 1N HCl, then dried over $MgSO_4$ filtered and evaporated. Recrystallization from a mixture of DCM – ethanol afforded **11h** as a beige solid (151 mg, 20%), mp.: 216-218 °C. ^{1}H NMR ($DMSO_{d6}$): δ 8.71 (1H, d d, J = 0.8, 1.3 Hz), 8.26 (1H, s br), 8.21 (1H, d, J = 1.3, 8.6 Hz), 8.16 (1H, d d, J = 0.8, 8.6 Hz), 7.63 (1H, s br), 5.43 (2H, s), 3.90 (2H, s), 1.58 (6H, s). ^{13}C NMR ($DMSO_{d6}$): δ 166.9, 145.4, 144.6, 133.7, 131.9, 129.1, 119, 113.9, 81.7, 78.7, 61.7, 22.5. Elemental analysis: ($C_{13}H_{15}N_5O_3$) Calc: C, 53.97; H, 5.23; N, 24.21. Found: C, 53.65; H, 5.51; N, 24.54.

Pharmacology

Animal treatment: All animal procedures conformed to the guidelines from Directive 2010/63/EU of the European Parliament on the protection of animals used for scientific purposes and the Portuguese law on animal welfare (Decreto-Lei 113/2013). Adult male NMRI mice were obtained from Harlan (Spain). Animals were maintained in macrolon cages (Tecniplast, Italy) with free access to food (2014 Teklad Global 14% Protein Rodent Maintenance, Envigo) and tap water under controlled environmental conditions in a colony room (12 hours light/dark cycle, room temperature: 22±2 ºC and relative humidity: 60±10%). Experiments were carried out during daylight hours. Animals were then given just water. Overnight fasted animals were administered compounds via oral route (gavage) at 8 mL/kg using animal feeding stainless steel needles (Perfectum, USA). For the 24 h time point the food was removed in the morning of the day of administration and compounds administered at the end of the afternoon of the same day. For ED_{50} determination doses administered were 0.001, 0.003, 0.01, 0.03 and 0.1 mg/kg in 10% (v/v) DMSO. The vehicle for other compound administrations was 0.5% (w/v) carboxymethylcellulose except for compound **2** that was 5% *N*,*N*-dimethylacetamide and 95% 2-hydroxypropyl-β-cyclodextrin (40% w/v in water). Fifteen minutes before sacrifice animals were anesthetized with 60 mg/kg pentobarbital sodium administered intraperitoneally. A fragment of liver, and brain without cerebellum were removed and put in plastic vials containing membrane buffer (3 mM $MgCl_2$, 1 mM EDTA, 50 mM Tris HCl pH 7.4). Tissues were stored at -30ºC until processed for analysis where tissues were thawed on ice and were homogenized in 10 volumes of membrane buffer with Heidolph Diax (position 5, 30 sec for livers and 20 sec for brains). FAAH activity was evaluated in these preparations.

Reagent and solutions: Anandamide [ethanolamine -1-3H-] (3H-AEA, 40–60Ci/mmol) and 2-monoleoyl glycerol (2-OG, 40-60 Ci/mmol) were obtained from American Radiochemicals (USA). 1-oleoyl-rac-glycerol (OG), arachidonylethanolamide (AEA), fatty acid free bovine serum albumin, and all other reagents were obtained from Merck (Germany). Optiphase Supermix was obtained from Perkin Elmer (USA).

Enzymatic assays: FAAH activity in vitro and in tissues preparations from treated animals was evaluated essentially as described in Kiss et al.[44] In brief, for compound evaluation in vitro reaction mix (total volume of 200 mL) contained: 2 µM AEA (2 µM AEA + 5 nM ^{3}H-AEA), 0.1% fatty acid free BSA (bovine serum albumin), 5 µg rat brain membrane preparation and the compound to evaluate in 1 mM EDTA, 10 mM Tris pH 7.6. After a 15 min pre-incubation period at 37 ºC, reaction was started by the addition of the substrate solution (cold AEA + radiolabelled AEA + BSA). Reaction was carried out for 10 min before termination. For tissues from treated animals the reaction contained 15 µg (brain) or 5 µg (liver) protein, no compound, and after a preincubation period of 10 min reaction was carried out for 10 min (brain) or 7 min (liver) before termination. Reactions were terminated by the addition of 400 mL activated charcoal suspension (8 g charcoal in 32 mL 0.5 M HCl in continuous agitation). After a 30 min incubation period at room temperature with agitation, charcoal was sedimented by centrifugation in microfuge (10 min at 13000 rpm). 200 µL of the supernatant were added to 800 µL Optiphase Supermix scintillation

cocktail previously distributed in 24-well plates. Counts per minute (cpm) were determined in a MicrobetaTriLux scintillation counter (Perkin Elmer). In each assay blanks (without protein) were prepared. The percentage of remaining enzymatic activity was calculated with respect to controls (no compound) and after blank subtraction. In some assays reaction was terminated by the addition of 400 µL chloroform – methanol (1:1 v/v). Reactions were vortex twice, left on ice for 5 min and were then centrifuged in microfuge (7 min at 7000 rpm). Counts per minute were determined in 200 µL of the supernatant as described above.

MAGL assay: MAGL activity was determined using cerebellar cytosol prepared from Wistar rats. In brief, cerebella were homogenised at 4 ºC in sodium phosphate buffer (50 mM, pH 8) containing 0.32 M sucrose. Homogenates were then centrifuged at 100,000 g for 60 min at 4 ºC. The supernatants (cytosol fractions) were collected and stored frozen in aliquots at -70 ºC until used for assay. Reaction contained, in a final volume of 200 µL, 100 µM test compound, 8 µg total protein, the substrate (2 µM 1-oleoyl-rac-glycerol and 5 nM 3H-2-OG), 0.1% fatty acid free BSA in 1 mM EDTA 10 mM TrisHCl, pH 7.2. Reaction was started with substrate after a 10 min preincubation period and was carried out for 8 min at 37 ºC until termination with 400 µL chloroform:methanol (1:1 v/v). Phase separation was achieved by centrifugation (7 min, 7000 r.p.m.in microfuge). 200 µL of the methanol phase were added to 800 µL Optiphase Supermix scintillation cocktail previously distributed in 24-well plates. Counts per minute (cpm) were determined in a MicrobetaTriLux scintillation counter (Perkin Elmer). In each assay blanks (without protein) were prepared. The percentage of remaining enzymatic activity was calculated with respect to controls (no compound) and after blank subtraction. Total protein was determined with the BioRad Protein Assay (BioRad) using a standard curve of BSA (50–250 mg/mL).

CE activity determination: The assay to evaluate the CEs activity was conducted in 96-well plates at 37 ºC using a modified method described by Wheelock et al.[45] Briefly, rat liver microsomes (8 µg/mL) were incubated for 15 min in a shaking water bath in the presence or in the absence of 10 µM of test compounds, in a final volume of 100 µL. Test compounds stock solutions (10 mM) were initially dissolved in dimethyl sulfoxide, but the final concentration of the solvent in the reaction medium was kept below 0.1%, which had no effect on CE activity. After 15 min incubation, the enzymatic reaction was initiated by the addition of 1 mM 4-nitrophenyl acetate (prepared in ethanol with less than 0.5% in final solution). Incubation occurred for 10 min in a shaking water bath at 37 ºC. The reaction was stopped by adding acetonitrile and the CE activity was measured at 405 nm using a spectrophotometer. The CE activity without test compounds was set at 100% and the remaining CE activity after incubation with test compounds was calculated relative to the control. All experiments were performed with samples in quadruplicate.

CYP450 metabolic stability assay: Stability of the test compounds was performed in liver microsomes in the presence and in the absence of NADPH. The stability was measured using the incubation mixture (100 µL total volume) contained 1mg/mL total protein, $MgCl_2$ 5 mM and 50 mM K-phosphate buffer. Samples were incubated in the presence and in the absence of NADPH 1 mM. Reactions were pre-incubated 5 min and the reaction initiated with the compound under test (5 µM for human liver microsomes and 50 µM for mouse liver microsomes). Samples were incubated for 60 min in a shaking water bath at 37 ºC. The reaction was stopped by adding 100 µL of acetonitrile. Samples were then centrifuged, filtered and supernatant injected in HLPC – MSD. Test compounds were dissolved in DMSO and the final concentration of DMSO in the reaction was below 0.5% (v/v). At T0 acetonitrile was added before adding the compound. All experiments were performed with samples in duplicate.

Keywords: BIA 10-2474 • Fatty acid amide hydrolase (FAAH) • Anandamide (AEA) • Pain • Target selectivity

References:

[1] M. K. McKinney, B. F. Cravatt, *Annu. Rev. Biochem.* **2005**, *74*, 411-432.
[2] B. F. Cravatt, D. K. Giang, S. P. Mayfield, D. L. Boger, R. A. Lerner, N. B. Gilula, *Nature* **1996**, 384, 83-87.
[3] D. M. Lambert, C. J. Fowler, *J. Med. Chem.* **2005**, *48*, 5059-5087.
[4] B. F. Cravatt, A. H. Lichtman, *Curr. Opin. Chem. Biol.* **2003**, *7*, 469-475.
[5] W. Tuo, N. Leleu-Chavain, J. Spencer, S. Sansook, R. Millet, P. Chavatte, *J. Med. Chem.* **2017**, *60*, 4-46.
[6] K. Ahn, M. K. McKinney, B. F. Cravatt, *Chem. Rev.* **2008**, *108*, 1687-1707.
[7] S. Vandevoorde, *Curr. Top. Med. Chem.* **2008**, *8*, 247-267.
[8] K. Ahn, D. S. Johnson, B. F. Cravatt, *Expert Opin. Drug Discov.* **2009**, *4*, 763-784.
[9] H. Deng, *Expert Opin. Drug Discov.* **2010**, *5*, 961-993.
[10] A. Lodola, R. Castelli, M. Mor, S. Rivara, *Expert Opin. Ther. Pat.* **2015**, *25*, 1247-1266.
[11] M. H. Bracey, M. A. Hanson, K. R. Masuda, R. C. Stevens, B. F. Cravatt, *Science* **2002**, *298*, 1793-1796.
[12] M. Mileni, D. S. Johnson, Z. Wang, D. S. Everdeen, B. Pabst, K. Bhattacharya, R. A. Nugent, S. Kamtekar, B. F. Cravatt, K. Ahn, R. C. Stevens, *Proc. Natl. Acad. Sci.* **2008**, *105*, 12820-12824.
[13] K. Ahn, D. S. Johnson, M. Mileni, D. Beidler, J. Z. Long, M. K. McKinney, E. Weerapana, N. Sadagopan, M. Liimatta, S. E. Smith, S. Lazerwith, C. Stiff, S. Kamtekar, K. Bhattacharya, Y. Zhang, S. Swaney, K. Van Becelaere, R. C. Stevens, B. F. Cravatt, *Chem. Biol.* **2009**, *16*, 411-420.
[14] M. Mileni, J. Garfunkle, J. K. DeMartino, B. F. Cravatt, D. L. Boger, R. C. Stevens, *J. Am. Chem. Soc.* **2009**, *131*, 10497-10506.
[15] M. Mileni, J. Garfunkle, C. Ezzili, F. S. Kimball, B. F. Cravatt, R. C. Stevens, D. L. Boger, *J. <med. Chem.* **2010**, *53*, 230-240.
[16] M. Mileni, S. Kamtekar, D. C. Wood, T. E. Benson, B. F. Cravatt, R. C. Stevens, *J. Mol. Biol.* **2010**, *400*, 743-754.
[17] C. Ezzili, M. Mileni, N. McGlinchey, J. Z. Long, S. G. Kinsey, D. G. Hochstatter, R. C. Stevens, A. H. Lichtman, B. F. Cravatt, E. J. Bilsky, D. L. Boger, *J. med. Chem.* **2011**, *54*, 2805-2822.
[18] M. Mileni, J. Garfunkle, C. Ezzili, B. F. Cravatt, R. C. Stevens, D. L. Boger, *J. Am. Chem. Soc.* **2011**, *133*, 4092-4100.
[19] K. Otrubova, M. Brown, M. S. McCormick, G. W. Han, S. T. O'Neal, B. F. Cravatt, R. C. Stevens, A. H. Lichtman, D. L. Boger, *J. Am. Chem. Soc.* **2013**, *135*, 6289-6299.
[20] D. L. Boger, H. Miyauchi, W. Du, C. Hardouin, R. A. Fecik, H. Cheng, I. Hwang, M. P. Hedrick, D. Leung, O. Acevedo, C. R. Guimaraes, W. L. Jorgensen, B. F. Cravatt, *J. Med. Chem.* **2005**, *48*, 1849-1856.
[21] M. Mor, S. Rivara, A. Lodola, P. V. Plazzi, G. Tarzia, A. Duranti, A. Tontini, G. Piersanti, S. Kathuria, D. Piomelli, *J. Med. Chem.* **2004**, *47*, 4998-5008.
[22] K. Ahn, D. S. Johnson, L. R. Fitzgerald, M. Liimatta, A. Arendse, T. Stevenson, B. F. Cravatt, *Biochemistry* **2007**, *46*, 13019-13030.
[23] J. M. Keith, R. Apodaca, W. Xiao, M. Seierstad, K. Pattabiraman, J. Wu, M. Webb, M. J. Karbarz, S. Brown, S. Wilson, B. Scott, C. S. Tham, L. Luo, J. Palmer, M. Wennerholm, S. Chaplan, J. G. Breitenbucher, *Bioorg. Med. Chem. Lett.* **2008**, *18*, 4838-4843.
[24] D. S. Johnson, K. Ahn, S. Kesten, S. E. Lazerwith, Y. Song, M. Morris, L. Fay, T. Gregory, C. Stiff, J. B. Dunbar Jr, M. Liimatta, D. Beidler, S. Smith, T. K. Nomanbhoy, B. F. Cravatt, *Bioorg. Med. Chem. Lett.* **2009**, *19*, 2865-2869.
[25] J. M. Keith, W. M. Jones, M. Tichenor, J. Liu, M. Seierstad, J. A. Palmer, M. Webb, M. Karbarz, B. P. Scott, S. J. Wilson, L. Luo, M. L. Wennerholm, L. Chang, M. Rizzolio, R. Rynberg, S. R. Chaplan, J. G. Breitenbucher, *ACS Med. Chem. Lett.* **2015**, *6*, 1204-1208.
[26] D. S. Johnson, C. Stiff, S. E. Lazerwith, S. R. Kesten, L. K. Fay, M. Morris, D. Beidler, M. B. Liimatta, S. E. Smith, D. T. Dudley, N. Sadagopan, S. N. Bhattachar, S. J. Kesten, T. K. Nomanbhoy, B. F. Cravatt, K. Ahn, *ACS Med. Chem. Lett.* **2011**, *2*, 91-96.
[27] J. P. Huggins, T. S. Smart, S. Langman, L. Taylor, T. Young, *Pain* **2012**, *153*, 1837-1846.
[28] H. R. Chobanian, Y. Guo, P. Liu, M. D. Chioda, S. Fung, T. J. Lanza, L. Chang, R. K. Bakshi, J. P. Dellureficio, Q. Hong, M. McLaughlin, K. M. Belyk, S. W. Krska, A. K. Makarewicz, E. J. Martel, J. F. Leone, L. Frey, B. Karanam, M. Madeira, R. Alvaro, J. Shuman, G. Salituro, J. L. Terebetski, N. Jochnowitz, S. Mistry, E. McGowan, R. Hajdu, M.

Rosenbach, C. Abbadie, J. P. Alexander, L. L. Shiao, K. M. Sullivan, R. P. Nargund, M. J. Wyvratt, L. S. Lin, R. J. DeVita, *ACS Med. Chem. Lett.* **2014**, *5*, 717-721.

[29] L. E. Kiss, D. A. Learmonth, C. Rosa, R. Noronha, P. N. Palma, P. Soares-da-Silva, A. Beliaev, WO2010074588, **2010**.

[30] A. Makriyannis, L. Pandarinathan, N. Zvonok, T. Parkkari, L. Chapman, (Northeastern University, Boston, USA) Int. PCT Pub. No. WO2009117444, **2009**.

[31] J. L. G. Nilsson, H. Sievertsson, R. Dahlbom, *Acta. Chem. Scand.* **1968**, *22*, 683-685.

[32] L. Boldrup, S. J. Wilson, A. J. Barbier, C. J. Fowler, *J. Biochem. Biophys. Methods* **2004**, *60*, 171-177.

[33] D. Piomelli, G. Tarzia, A. Duranti, A. Tontini, M. Mor, T. R. Compton, O. Dasse, E. P. Monaghan, J. A. Parrott, D. Putman, *CNS Drug Rev.* **2006**, *12*, 21-38.

[34] D. Russo, G. B. Whanon, W. Maton, T. Eszenyi, (BIAL – Portela & Cª., S.A., S. Romão and S. Mamede, Portugal), Int. PCT Pub. No. WO2014017938, **2014**.

[35] A. Kerbrat, J. C. Ferre, P. Fillatre, T. Ronziere, S. Vannier, B. Carsin-Nicol, S. Lavoue, M. Verin, J. Y. Gauvrit, Y. Le Tulzo, G. Edan, *N. Engl. J. Med.* **2016**, *375*, 1717-1725.

[36] CSST (2016) "*Report by the Temporary Specialist Scientific Committee (TSSC): FAAH (Fatty Acid Amide Hydrolase)", on the causes of the accident during a Phase 1 clinical trial in Rennes in January* 2016" to be found under http://ansm.sante.fr/var/ansm_site/storage/original/application/744c7c6daf96b141bc9509e2f85c227e.pdf, **2016**.

[37] A. C. M. van Esbroeck, A. P. A. Janssen, A. B. Cognetta III, D. Ogasawara, G. Shpak, M. van der Kroeg, V. Kantae,, M. P. Baggelaar, F. M. S. de Vrij, H. Deng, M. Allarà, F. Fezza, Z. Lin, T. van der Wel, M. Soethoudt, E. D. Mock, H. den Dulk, I. L. Baak, B I. Florea, G. Hendriks, L. De Petrocellis, H. S. Overkleeft, T. Hankemeier, C. I. De Zeeuw, V. Di Marzo, M. Maccarrone, B. F. Cravatt, S. A. Kushner, M. van der Stelt, *Science* **2017**, *356*, 1084–1087.

[38] R. J. Richardson, N. D. Hein, S. J. Wijeyesakere, J. K. Fink, G. F. Makhaeva, *Chem. Biol. Interact.* **2013**, *203*, 238–244.

[39] M. J. Bonifácio, C. Lopes, N. Pires, A. I. Loureiro, P. Moser, P. Soares-da-Silva, *pA₂ online* **2017**, *16*, 203P.

[40] A. I. Loureiro, C. Lopes, M. J. Bonifácio, P. Moser, P. Soares-da-Silva, *pA₂ online* **2017**, *16*, 216P.

[41] A. I. Loureiro, C. Lopes, M. J. Bonifácio, P. Moser, P. Soares-da-Silva, *pA₂ online* **2017**, *16*, 212P.

[42] J. F. Rocha, A. Santos, D. Chassard, A. Patat, A. Astruc, A. Falcão, H. Gama, P. Soares-da-Silva, *pA₂ online* **2017**, *16*, 178P.

[43] H. Gama, M. Vieira, J. Graça, D. Chassard, J. Massano, H. Charfi, A. Patat, A. Santos, J. F. Rocha, P. Soares-da-Silva, *pA₂ online* **2017**, *16*, 188P.

[44] L. E. Kiss, H. S. Ferreira, A. Beliaev, L. Torrão, M. J. Bonifácio, D. A. Learmonth, *Med. Chem. Comm.* **2011**, *2*, 889-894.

[45] C. E. Wheelock, T. F. Severson, B. D. Hammock, *Chem. Res. Toxicol.* **2001**, 1563-1572.

Entry for the Table of Contents

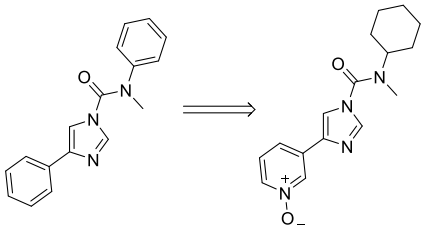

8b

ED_{50} >> 1 mg/kg

8l (BIA 10-2474)

$ED_{50(liver)}$ = 7 µg/kg
$ED_{50(brain)}$ = 27 µg/kg

Herein we describe the discovery of BIA 10-2474, a novel inhibitor of Fatty Acid Amide Hydrolase (FAAH). BIA 10-2474 was developed from a weak in vitro hit. The paper includes a short SAR of the series and then presents the excellent pharmacodynamic effect of BIA 10-2474 such as ED_{50} values in the low µg/kg range (mouse, p.o.) and significant inhibition up to 48 h post-dose (mouse, p.o., 0.1 mg/kg).